

Silver nanoparticles induced genotoxicity and oxidative stress in tomato plants

Fazilet Özlem ÇEKİÇ^{1*}, Sefa EKİNCİ¹, Müslüm Süleyman İNAL², Dilek ÜNAL²

¹Department of Biology, Faculty of Science and Letters, Aksaray University, Aksaray, Turkey

²Department of Molecular Biology and Genetics, Faculty of Science and Letters, Bilecik Seyh Edebali University, Bilecik, Turkey

Received: 12.08.2016 • Accepted/Published Online: 28.10.2016 • Final Version: 10.11.2017

Abstract: Among nanoparticles, silver nanoparticles (AgNPs) are intensively used in many materials owing to their antibacterial effects. In the present study different concentrations of AgNPs in Hoagland solution were applied to tomato seedlings. Total chlorophyll content, relative water content (RWC), antioxidant enzyme activities, and malondialdehyde content (MDA) as well as the genomic template stability (GTS) were analyzed. The intersimple sequence repeat polymerase chain reaction assay (ISSR-PCR) was used to determine the genotoxic effects of AgNPs on DNA. RWC did not change under AgNPs treatments; however, total chlorophyll content was significantly reduced by AgNPs applications. ISSR profiles demonstrated a consistent increase in polymorphic bands by the increase in the concentration of AgNPs. GTS value was also reduced depending on the concentration of AgNPs. SOD and APX activities were increased under low AgNPs treatments; however, these activities were decreased under high concentrations of AgNPs treatments. Tomato plants could be sensitive to AgNPs within the increase in MDA content in all of the AgNPs treatments. AgNPs nanotoxicity could be quite dose-dependent. AgNPs could also have negative effects on tomato plants by enhancing DNA damage and lipid peroxidation.

Key words: AgNP, antioxidant enzymes, ISSR-PCR, *Solanum lycopersicum* L.

1. Introduction

Silver nanoparticles (AgNPs) are widely used among other nanoparticles in many industries within a wide range of consumer products because of their antibacterial and biocidal properties (Thuesombat et al., 2014). In recent years, the significant increase in the consumption of nanoparticles has caused environmental, health, and safety concerns regarding their potential effects (Ma et al., 2010; Pokhrel and Dubey, 2013). Nanoparticles could uncertainly spread to the environment. However, the interaction between AgNPs and plant systems is still not well known (Patlolla et al., 2012; Song et al., 2013).

AgNPs are known to be absorbed by plants and could interact with intracellular parts causing water imbalances, cell damage, and decreases in photosynthesis (Kumari et al., 2009; Qian et al., 2013). They are also reported to have genotoxic effects on plant cells, inducing chromosomal aberrations and micronucleus induction (Patlolla et al., 2012). However, the impacts of nanoparticles on plants can vary according to the nanoparticle concentration, size, chemical properties, and plant species (Ma et al., 2010; Thuesombat et al., 2014).

Nanotoxicity could lead to oxidative stress and previous studies indicate that AgNPs could induce toxicity due to their effect on reactive oxygen species

(ROS) formation (Qian et al., 2013; McShan et al., 2014). The imbalance of ROS production and antioxidant activity can cause oxidative damage, and plants cope with this oxidative damage by their antioxidant defense mechanism (Saed-Moucheshi et al., 2014). Previously, studies on the genotoxicity of nanoparticles have used cell viability, chromosome aberration, or micronucleus assays to identify the genotoxic effect, and comet analysis for detecting the DNA damage in different plant species (Kumari et al., 2009; Kumari et al., 2011; Patlolla et al., 2012; Ghosh et al., 2012). However, these methods are very restricted for identifying the genotoxic effects of nanoparticles at the DNA level. DNA-based techniques are sensitive and selective assays that help to determine the genotoxic effects of environmental pollutants on DNA. One of these methods used for these aims is the intersimple sequence repeat (ISSR)-PCR assay. ISSR-PCR uses as primer microsatellite repeats (Zietkiewicz et al., 1994). The ISSR-PCR method is more sensitive than the random amplified polymorphic DNA assay (RAPD) (Correia et al., 2014; Bajpai et al., 2015), because of the exhibiting specificity of the sequence-tagged-site markers and high ratio of reproducibility potential owing to the use of longer primers (16–25 bp).

* Correspondence: faziletozlem@gmail.com

The potential effects of AgNPs on plants, especially on edible crop plants, should be evaluated before their widespread application (Kumari et al., 2009; Lee et al., 2012; Qian et al., 2013). *Solanum lycopersicum* L. is an important edible plant around the world; hence the aim of our study was to examine the effects of AgNPs (<100 nm) on DNA damage, genomic template stability, the antioxidant defense system, and lipid peroxidation in tomato plants.

2. Materials and methods

2.1. Growth conditions and stress treatment

The seeds of *Solanum lycopersicum* L. cv. H-2274 were obtained from the Anatolia Agricultural Research Institute in Eskişehir, Turkey. Seeds of tomato plants were surface sterilized with 0.5% sodium hypochlorite solution for 5 min, and washed thoroughly with sterile water, and then they were transferred to individual pots filled with perlite. They were grown in the growth chamber under controlled conditions (16 h/8 h light/dark photoperiod at 26 °C/22 °C, photosynthetic photon flux density of 350 $\mu\text{mol m}^{-2} \text{s}^{-1}$ and a relative humidity of 60%–70%). The seedlings were watered regularly with ½ Hoagland solution (Hoagland and Arnon, 1950). After 2 months the plants were exposed to 0, 10, 20, 40, 80 mg/L AgNPs within Hoagland solution (Sigma-H2395) for 2 weeks. The concentration of AgNPs was decided according to Panda et al. (2011). AgNPs were purchased from Sigma-Aldrich (7440-22-4, No. 576832). According to the manufacturer's specifications, the particle size was below 100 nm with a thermal resistance of 1.59 Wm/cm at 20 °C with a surface area of 5.0 m²/g. Scanning electron microscope (SEM) images of AgNPs are shown as supplementary materials (Figure S1). The images were obtained by using the Fei Quanta FEG 250 SEM instrument located at Aksaray University. The experiment was performed as a randomized block design. Leaf samples were taken from the second well-developed leaves of individual plants per treatment from each individual pot, and three replications were used for each analysis. The leaves (0.2 g, 0.5 g) were frozen in liquid nitrogen and then stored at –80 °C until analyses. All of the spectrophotometric analyses were conducted on a Thermo Scientific Genesys 10s UV-VIS spectrophotometer.

2.2. Relative water content (RWC)

The RWC of leaves was determined according to Barrs and Weatherley (1962). It was defined by the following formula:

$$\text{RWC (\%)} = \frac{[(\text{FW} - \text{DW})/(\text{TW} - \text{DW})] \times 100}{100}$$
 where FW is initial fresh weight, TW is turgid fresh weight, and DW is dry weight.

2.3. Total chlorophyll content

Total chlorophyll content was assayed according to (Zhang et al., 2013) Arnon (1949). The chlorophyll concentrations were calculated by the following equation:

$$[\text{Chlorophyll a + b}] (\text{mg/g}) = [19.54 E^{646.6} + 8.29 E^{663.6}] \times V/1000 \times W$$
 where V = volume of the extract (mL); W = Weight of fresh leaves (g) (Porra, 2002).

2.4. Enzyme extractions and assays

First 0.5-g leaf samples were homogenized (Heidolph 12 F) in 50 mM sodium phosphate buffer (pH 7.8, 2% (w/v) polyvinylpyrrolidone (PVP) and 1 mM EDTA), and then centrifuged at 12,000 $\times g$ for 10 min at 4 °C. Supernatants of the homogenates were used for enzyme activity and protein content assays. BSA was used as a standard for the assay of total protein contents (Bradford, 1976).

Superoxide dismutase (SOD; EC 1.15.1.1) activity was measured spectrophotometrically according to Beyer and Fridowich (1987). Enzyme extracts were incubated at 25 °C under light for 10 min in a 50 mM Na phosphate buffer (pH 7.8) containing 33 μM NBT, 10 mM L-methionine, 0.66 mM EDTA, and 0.0033 mM riboflavin. The activity was determined at 560 nm. One unit of SOD activity was expressed as the quantity that causes 50% inhibition of the photochemical reduction of NBT.

APX activity (APX; EC 1.11.1.11) was performed according to Nakano and Asada (1981). APX activity was analyzed in a reaction mixture containing 50 mM Na-phosphate buffer (pH 7.0), 0.5 mM ascorbate, 0.1 mM EDTANa₂, and 1.2 mM H₂O₂. The reaction was started following the addition of H₂O₂. The oxidation rate of ascorbic acid was determined by measuring the decrease in absorbance at 290 nm. The concentration of oxidized ascorbate was calculated by using an extinction coefficient of 2.8 mM⁻¹ cm⁻¹.

Catalase (CAT; EC 1.11.1.6) activity was measured according to Bergmeyer (1970). The activity was assayed in the reaction mixture containing 0.05 M Na phosphate buffer (pH 7, 0.1 mM EDTA) and 3% H₂O₂. The disappearance of H₂O₂ was measured at 240 nm. One unit of CAT activity was defined as 1 $\mu\text{mol H}_2\text{O}_2$ destroyed per minute.

Glutathione reductase (GR, EC 1.6.4.2) activity was assayed by following the oxidation of NADPH₂ (Carlberg and Mannervik, 1985). The reaction mixture contained 0.1 M potassium phosphate buffer (pH 7), 20 mM GSSG, 2 mM NADPH₂ (dissolved in Tris-HCl buffer, pH 7), and enzyme extract. The reaction was initiated by the addition of GSSG, and NADPH oxidation was detected spectrophotometrically at 340 nm.

2.5. Lipid peroxidation

Lipid peroxidation was performed by analyzing MDA content (Karabal et al., 2003). First 0.2 g of leaf samples were homogenized in 1 mL of 5% trichloroacetic acid solution (TCA) and then centrifuged at 12,000 rpm for 15 min. Supernatant of the leaf extract and 0.5% thiobarbituric acid (TBA) (dissolved in 20% TCA solution) were mixed and incubated at 96 °C for 25 min. After the tubes were cooled in an ice bath, they were centrifuged at 10,000 rpm for 5

min. The supernatant was then measured at 532 and 600 nm. MDA content was calculated by using the extinction coefficient ($155 \text{ mM}^{-1} \text{ cm}^{-1}$).

2.6. DNA isolation

Total DNA was isolated from *S. lycopersicum* roots by micropreparation (Fulton et al., 1995). After DNA isolation, DNA yield and quality were quantified with a nanodrop spectrophotometer (BioSpec-nano, Japan) and visualized on 1% agarose gel.

2.7. ISSR PCR protocol

Amplification of the genomic DNA for ISSR PCR was performed in a 25- μL reaction mixture (25 ng of genomic DNA, 2.5 μL of 10X Taq buffer, Thermo, 1 μL of 25 mM MgCl_2 , 0.5 μL of primer, 2 μL of 1.25 mM dNTP, 0.25 μL of Taq polymerase). Next 15 different ISSR primers were used for ISSR-PCR (Table 1). Amplification was assayed in a Biorad T100 Thermal Cycler as 1 cycle at 94 °C for 2 min and 40 cycles at 94 °C for 30 s, annealing at 47–52 °C for 45 s, and extension at 72 °C for 45 s. A final extension step was performed for 20 min. The sequence and annealing temperature of each primer are shown in Table 1.

For visualizing the PCR product, 12 μL of each sample was electrophoresed on agarose gel (1.5%) in TBE buffer at 80 V for 1.5 h. Ethidium bromide was used for staining the gel and it was photographed by Gel Logic 212 Pro Gel documentation systems.

2.8. Genomic template analysis

ISSR profiles were expressed as +1 arbitrary score. The average of each experimental group of AgNPs was given. GST (%) was calculated as follows:

$$\text{GST} = 100 - (100a/n)$$

a means the average number of the differences in DNA profiles; *n* means the number of bands that were selected through control profiles of DNA (Unal and Silah, 2013).

2.9. Statistical analysis

The effect of AgNPs was determined by one-way analysis of variance (ANOVA) using SPSS 17.0. The means of the treatments were compared by least significant difference (LSD) test ($P < 0.05$). The spread of values is shown in the figures as standard errors of the means.

3. Results

The highest RWC was found in the control plants, whereas the lowest RWC was detected in 20 mg/L AgNPs-treated plants, 6.81% lower than that of the control plants. However, we did not find any remarkable difference between the AgNP applications (Figure 1).

As shown in Figure 2, total chlorophyll content was decreased by 80 mg/L AgNPs (69.41%), 40 mg/L AgNPs (20.89%), 20 mg/L AgNPs (3.16%), and 10 mg/L AgNPs (9.88%) treatments when compared to the control plants ($P < 0.05$).

The activities of SOD, CAT, APX, and GR are shown in Figures 3–6. SOD activity was increased in 10 (30.74%) and 20 (4.58%) mg/L AgNPs applications as compared to the control plants (Figure 3). The highest SOD activity was found in the 10 mg/L AgNPs treatment. However, SOD activity was decreased in the 40 (8.21%) and 80 (16.45%) mg/L AgNPs treatments when compared to the control plants.

Table 1. ISSR primers used for PCR amplification.

ISSR primers	Sequence (5'-3')	Annealing temperature (°C)
808	(AG) ₇ AAGC	51
807	(AG) ₈ T	47
809	(AG) ₈ G	53
810	(GA) ₈ T	49
818	(CA) ₈ G	51
826	(AC) ₈ C	49
828	(TG) ₈ A	49
830	(TG) ₈ G	49
873	(GACA) ₄	54
880	(GGAGA) ₂ GGAG	48
866	(CTC) ₆	49
842	(GAGA) ₄ T	49
868	(GAA) ₆	52
813	(CTCT) ₄ T	51
890	GGA(GAG) ₂ AGG	51

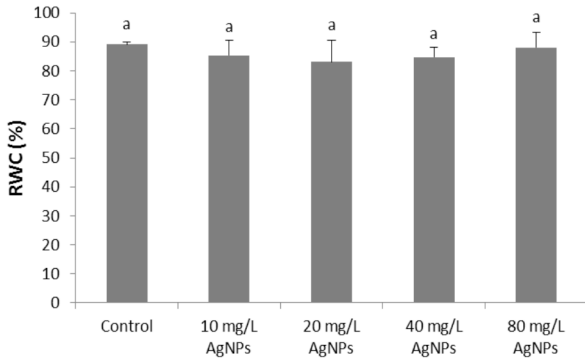


Figure 1. The effects of silver nanoparticles on relative water content (RWC) of *S. lycopersicum* L. Vertical bars indicate the mean of three replicates \pm standard errors (\pm SE) and values sharing a common letter are not significantly different at $P < 0.05$.

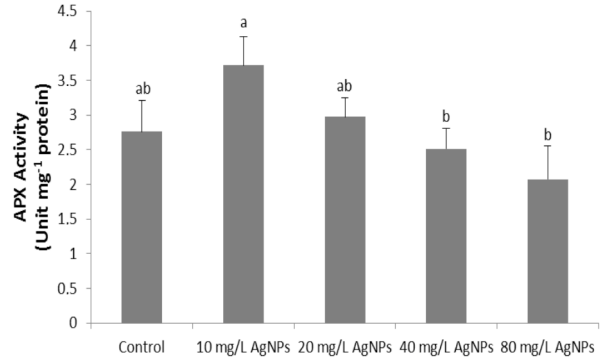


Figure 4. The effects of silver nanoparticles on APX activity in the leaves of *S. lycopersicum* L. Vertical bars indicate the mean of three replicates \pm standard errors (\pm SE) and values sharing a common letter are not significantly different at $P < 0.05$.

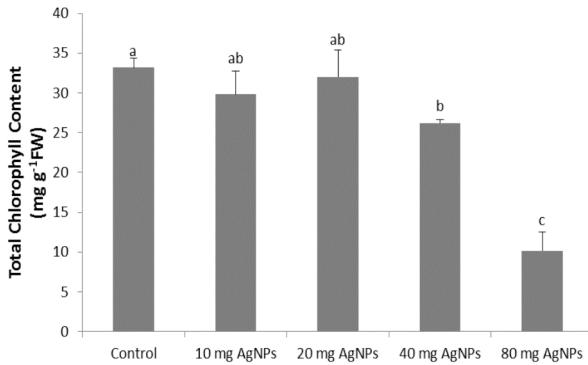


Figure 2. The effects of silver nanoparticles on total chlorophyll content of *S. lycopersicum* L. Vertical bars indicate the mean of three replicates \pm standard errors (\pm SE) and values sharing a common letter are not significantly different at $P < 0.05$.

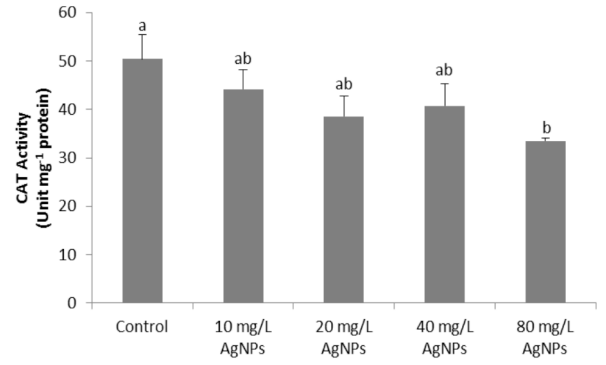


Figure 5. The effects of silver nanoparticles on CAT activity in the leaves of *S. lycopersicum* L. Vertical bars indicate the mean of three replicates \pm standard errors (\pm SE) and values sharing a common letter are not significantly different at $P < 0.05$.

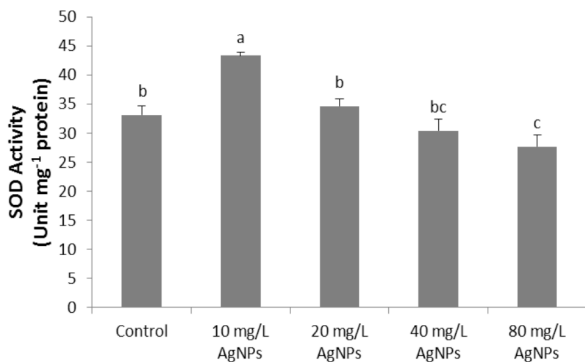


Figure 3. The effects of silver nanoparticles on SOD activity in the leaves of *S. lycopersicum* L. Vertical bars indicate the mean of three replicates \pm standard errors (\pm SE) and values sharing a common letter are not significantly different at $P < 0.05$.

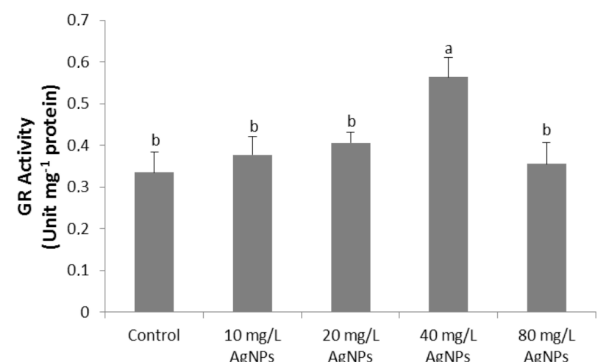


Figure 6. The effects of silver nanoparticles on GR activity in the leaves of *S. lycopersicum* L. Vertical bars indicate the mean of three replicates \pm standard errors (\pm SE) and values sharing a common letter are not significantly different at $P < 0.05$.

Similar to SOD activity, the highest APX activity was found in the 10 mg/L AgNPs treatment. APX activity was increased in the 10 mg/L AgNPs (34.66%) and 20 mg/L AgNPs (7.77%) applications; however, the 40 (8.89%) and 80 mg/L AgNPs (24.79%) treatments decreased APX activity when compared to the control plants (Figure 4).

The highest CAT activity was found in the control plants (Figure 5). The 10 (12.27%), 20 (23.44%), 40 (19.18%), and 80 mg/L AgNPs (33.48%) treatments decreased CAT activity, when compared to the control plants.

As shown in Figure 6, the highest GR activity was found in the 40 mg/L AgNPs application (68.69%). Moreover, the 10 (12.76%), 20 (21.46%), and 80 mg/L AgNPs (6.45%) caused an increase in GR activity as compared to the control plants ($P < 0.05$).

Lipid peroxidation was demonstrated as MDA content. The lowest MDA content was found in the control plants. We found a significant increase in MDA content under the 20 (80.47%), 40 (72.82%), and 80 mg/L AgNPs (79.62%) treatments ($P < 0.05$; Figure 7).

Ten ISSR primers indicated polymorphic bands. In our study, a total of 186 bands were detected in the presence and absence of AgNPs. Table 2 explains the differences observed in ISSR profiles as appearance/disappearance in bands and decrease/increase of band densities (Figure S2). The highest number of band appearance/disappearance was detected in samples treated with 80 mg/L AgNPs within all of the ten primers used.

According to the ISSR assay, the difference in GTS between the control and 10 mg/L AgNPs treatment

was 67.45%. The lowest value of GTS (18.61%) was also observed in the roots of *S. lycopersicum* treated with 80 mg/L AgNPs. As shown in Table 3, GTS value was reduced by the increase in AgNPs concentration.

4. Discussion

Previous reports indicate that AgNPs could have adverse physiological effects in different plants. The increase in the concentration of AgNPs could cause a reduction in growth in different plants according to AgNPs penetration and transport to the plant tissues (Qian et al., 2013; Thuesombat et al., 2014; Vannini et al., 2014; Nair and Chung, 2015). However, in a previous report (Sharma et al., 2012), it was declared that AgNPs could enhance growth by modulating the antioxidant status in *Brassica juncea*. Therefore, the effects of nanoparticles should be well evaluated before their widespread application.

Relative water content (RWC) was analyzed to understand the impact of AgNPs on water status in the leaves of tomato plants. Previously, it was mentioned that *L. esculentum* is sensitive to AgNPs treatments (Ravindran et al., 2012). According to our RWC results, AgNPs did not affect significantly the water status of *S. lycopersicum*. We also analyzed total chlorophyll content to evaluate nanotoxicity. Previous studies demonstrated that AgNPs decreased total chlorophyll content in *Arabidopsis thaliana* (Qian et al., 2013), *Lycopersicon esculentum* (Song et al., 2013), *Oryza sativa* (Nair and Chung, 2014a), and *Vigna radiata* (Nair and Chung, 2015). These studies are parallel to our study; we found a remarkable decrease in total

Table 2. The effects of silver nanoparticles on ISSR bands in the roots of *S. lycopersicum* L., a: appearance band number, b: disappearance band number, c: decreased band intensity, d: increased band intensity.

Primers	Control	AgNPs application concentration															
		10 mg/L AgNPs				20 mg/L AgNPs				40 mg/L AgNPs				80 mg/L AgNPs			
		a	b	c	d	a	b	c	d	a	b	c	d	a	b	c	d
ISSR810	4	0	2	0	0	1	2	0	0	0	3	0	1	0	3	0	0
ISSR826	4	0	0	0	0	1	2	0	2	0	2	0	1	0	2	0	1
ISSR842	1	0	0	0	0	0	0	0	1	0	1	0	0	0	0	0	1
ISSR830	3	1	1	1	0	0	0	2	0	0	3	0	0	0	1	2	0
ISSR808	6	3	0	1	2	0	0	0	1	0	5	0	1	3	0	0	1
ISSR818	3	0	1	0	0	2	2	0	0	0	3	0	0	6	2	0	0
ISSR890	6	0	3	0	0	0	5	0	0	0	4	0	0	0	4	0	0
ISSR809	5	0	0	0	1	1	0	1	0	0	1	2	0	3	0	0	2
ISSR807	6	0	2	0	2	2	2	0	1	1	3	1	0	3	3	0	3
ISSR880	5	1	0	0	1	1	0	0	2	0	1	2	1	4	1	0	1
Total bands	43	41				38				18				46			
a+b+c+d		22				31				36				46			

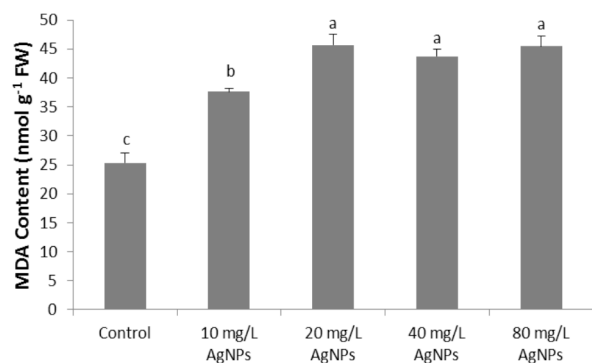


Figure 7. The effects of silver nanoparticles on lipid peroxidation in the leaves of *S. lycopersicum* L. Vertical bars indicate the mean of three replicates ± standard errors (±SE) and values sharing a common letter are not significantly different at P < 0.05.

chlorophyll content especially in high concentration AgNPs treatment, and this result could cause an inhibition in photosynthesis.

AgNPs could induce oxidative stress and reactive oxygen species (ROS) levels (Nair and Chung, 2014a, 2014b, 2015). ROS are known to be highly toxic and cause cell damage, chromosomal aberrations, and micronucleus induction (Patlolla et al., 2012; Pokhrel and Dubey, 2013). It is also known that the toxicity mechanisms of various nanoparticles are related to the imbalance between the production and the scavenging of ROS in the cellular components of plants (Oukarroum et al., 2013; Yasur and Randi, 2013). The antioxidant defense mechanism is very important in response to ROS toxicity. SOD is the first line of the defense mechanism and scavenges superoxide radicals (Bowler et al., 1992; Fatima and Ahmad, 2005). An increase in SOD activity of *L. esculentum* was reported in AgNPs treated plants (Song et al., 2013). In *Ricinus communis*, AgNPs treatment enhanced SOD activity up to 1.000 mg/L application; however, it was decreased in 2.000 mg/L AgNPs-treated plants (Yasur and Rani, 2013). Parallel to these studies, high concentration of AgNPs caused a reduction in SOD activity in tomato plants. In the present study, SOD activity also showed a negative correlation with lipid peroxidation rate. Our results indicate that the decline in SOD activity may cause damage to membranes due to increased lipid peroxidation formation in cellular components.

APX and CAT are other key enzymes in the antioxidant mechanism. They are responsible in the conversion of H₂O₂ into H₂O and molecular O₂. In *B. juncea*, it was reported that APX and CAT activities were increased under high AgNPs concentrations (Sharma et al., 2012). However, in the present study, APX activity was increased by 10 and 20 mg/L AgNPs but decreased by 40 and 80 mg/L AgNPs

Table 3. Changes in genomic template stability (GTS%) for 9 ISSR primers in AgNPs-treated *S. lycopersicum* L. roots.

AgNPs-treated groups	GTS ratio (%)
10 mg/L AgNPs	67.45
20 mg/L AgNPs	51.13
40 mg/L AgNPs	37.21
80 mg/L AgNPs	18.61

applications; this decrease could be due to the toxicity of AgNPs. Allen et al. (1994) demonstrated that APX activity could be enhanced by treating with H₂O₂. As in our study, the increase in SOD activity under 10 and 20 mg/L AgNPs treatments could lead to H₂O₂ generation leading to induced APX activity. Furthermore, the increase in APX activity could help to cope with the cell damage by reducing the H₂O₂ level. Moreover, in our study CAT activity was decreased under all of the AgNP applications. In a previous study, *R. communis* plants showed a decrease in CAT activity under low concentration of AgNPs, but an increase was mentioned in high concentration of AgNPs (Yasur and Rani, 2013). Our results indicate that in *S. lycopersicum* APX activity could be more effective than CAT in the conversion of H₂O₂ under low concentration of AgNPs.

According to SOD, APX, and CAT activities, it can be said that *S. lycopersicum* could be negatively affected especially by 40 and 80 mg/L AgNPs concentrations. In *Pelargonium* SOD, APX, and CAT activities were mentioned to be increased by dose-dependent application of nanosilver; however, high dose treatment significantly decreased the antioxidant enzyme activities (Hatami and Ghorbanpour, 2014). In the stress response, GR also has an important role in the ascorbate–glutathione cycle by converting the oxidized glutathione to glutathione. In our study, unlike the other enzyme activities, GR activity was increased under AgNPs applications when compared to control groups. In *B. juncea* GPX was reported to be enhanced by AgNPs treatments. This increase could be a reason for the role of glutathione in various metabolic pathways.

The decomposition product of the polyunsaturated fatty acids, MDA, is produced naturally as a result of lipid peroxidation and is often used as an indicator of oxidative damage at the cellular level (Mittler, 2002). In the present study, all concentrations of AgNPs caused a significant increase in MDA content as compared to control plants. The increase in MDA content may indicate silver nanotoxicity, especially under high AgNPs treatments. Parallel to our study, AgNPs treatment increased MDA

content in *O. sativa* (Nair and Chung, 2014a) in *V. radiata*; however, no significant change was mentioned upon different concentrations of AgNPs (Nair and Chung, 2015). Moreover, in our study the increase in antioxidant enzymes seems to be insufficient to overcome nanotoxicity, depending on the concentration of AgNPs.

The intersimple sequence repeat (ISSR) technique is very convenient for finding out the mutational effects of heavy metals and other environmental pollutants (Correia et al., 2014; Bajpai et al., 2015). The ISSR-PCR technique uses generally 16–25 bp long primers for a single PCR reaction showing multiple genomic loci from microsatellites for amplifying primarily the inter-SSR sequences in different size (Bornet and Branchard, 2001). In our study, we used the ISSR-PCR technique to determine the genotoxicity induced by AgNPs.

Genomic template stability (GTS) is known to be related to DNA damage (Sukumaran and Grant, 2013). Therefore, it has been used as a parameter for comparison of the genotoxic damage expressed in ISSR and RAPD profiles (Atienzar et al., 1999; Correia et al., 2014). In our study, GTS was decreased by different concentrations of AgNPs. This decrease might be attributed to increases in oxidative stress depending on the dose application. Previous studies showed that AgNPs have genotoxic effects in plant cells due to the induced oxidative stress

or generation of ROS (Kumari et al., 2011). Panda et al. (2011) also demonstrated that AgNPs induced cell death and DNA damage via generation of ROS. Similarly, our ISSR profile results indicate that AgNPs toxicity is related to the decline in antioxidant capacity and the increase in lipid peroxidation in tomato plants.

In conclusion, in tomato plants, high doses of AgNPs resulted in decreases in antioxidant enzyme activities. Treatment with high-dose AgNPs affects the template activity of DNA, and this impact could be due to damage in DNA. In addition, we suggest ISSR marker as a good tool for detecting the effect of AgNPs on DNA profiles. According to our results, we can conclude that AgNPs could cause toxicity to tomato plants via enhancing DNA damage and lipid peroxidation. Silver nanotoxicity can be positively dose-dependent. In this respect it can be said that tomato plants could be sensitive to AgNPs application. However, further studies should be done to evaluate the effects of AgNPs based on the interaction of nanoparticle size with plant species, and especially the effects of AgNPs on crop plants should be particularly identified.

Acknowledgment

The authors would like to thank to Aksaray University Research Foundation (Grant number: 2014-036).

References

- Arnon DI (1949). Copper enzymes in isolated chloroplasts. Polyphenoloxidase in *Beta vulgaris*. *Plant Physiol* 24: 1-15.
- Allen RD, Gupta SA, Webb RP, Holaday AS (1994). Protection of plants from oxidative stress using SOD transgenes: interactions with endogenous enzymes. In: Asada K, Yoshikawa T, editors. *Frontiers of Reactive Oxygen Species in Biology and Medicine*. Amsterdam, Netherlands: Excerpta Medica, pp. 321-322.
- Atienzar FA, Conradi M, Evenden AJ, Jha AN, Depledge MH (1999). Qualitative assessment of genotoxicity using random-amplified polymorphic DNA: comparison of genomic template stability with key fitness parameters in *Daphnia magna* exposed to benzo[a]pyrene. *Environ Toxicol Chem* 18: 2275-2282.
- Bajpai R, Shukla V, Singh N, Rana TS, Upreti DK (2015). Physiological and genetic effects of chromium (+VI) on toxictolerant lichen species, *Pyxine coccoides*. *Environ Sci Pollut Res* 22: 3727-3738.
- Barrs HD, Weatherley PE (1962). A re-examination of the relative turgidity technique for estimating water deficit in leaves. *Aust J Biol Sci* 15: 413-428.
- Bergmeyer N (1970). *Methoden der Enzymatischen Analyse*. Berlin, Germany: Akademie Verlag.
- Beyer WF, Fridowich I (1987). Assaying for superoxide dismutase activity: some large consequences of minor changes in conditions. *Anal Biochem* 161: 559-566.
- Bornet B, Branchard M (2001). Nonanchored Inter Simple Sequence Repeat (ISSR) markers: reproducible and specific tools for genome fingerprinting. *Plant Mol Biol Report* 19: 209-215.
- Bowler C, Van Montagu M, Inzé D (1992). Superoxide dismutase and stress tolerance. *Ann Rev Plant Physiol Plant Mol Biol* 43: 83-116.
- Bradford MM (1976). A rapid and sensitive method for the quantization of micro-gram quantities of protein utilizing the principle of the protein-dye binding. *Anal Biochem* 72: 248-254.
- Carlberg I, Mannervik B (1985). Glutathione reductase. *Methods Enzymol* 113: 484-490.
- Correia S, Matos M, Ferreira V, Martins N, Gonçalves S, Romano A, Pinto-Carnide O (2014). Molecular instability induced by aluminum stress in *Plantago* species. *Mutat Res - Genet Toxicol Environ Mutagen* 770: 105-111.
- Dimkpa CO, Mclean JE, Martineau N, Britt DW, Haverkamp R, Anderson AJ (2013). Silver nanoparticles disrupt wheat (*Triticum aestivum* L.) growth in a sand matrix. *Environ Sci Technol* 47: 1082-1090.
- Fatima RA, Ahmad M (2005). Certain antioxidant enzymes of *Allium cepa* as biomarkers for the detection of toxic heavy metals in wastewater. *Sci Total Environ* 346: 256-273.

- Fulton TM, Chunwongse J, Tanksley SD (1995). Microprep protocol for extraction of DNA from tomato and other herbaceous plants. *Plant Mol Biol Report* 13: 207-209.
- Ghosh M, Manivannan J, Sinha S, Chakraborty A, Mallick SK, Bandyopadhyay M, Mukherjee A (2012). In vitro and in vivo genotoxicity of silver nanoparticles. *Mutat Res* 749: 60-69.
- Hoagland DR, Arnon DI (1950). The water culture method for growing plants without soil. *Calif Agric Exp Stn* 347: 1-39.
- Hatami M, Ghorbanpour M (2014). Defense enzyme activities and biochemical variations of *Pelargonium zonale* in response to nanosilver application and dark storage. *Turk J Biol* 38: 130-139.
- Karabal E, Yücel M, Öktem HA (2003). Antioxidant responses of tolerant and sensitive barley cultivars to boron toxicity. *Plant Sci* 164: 925-933.
- Kumari M, Khan SS, Pakrashi S, Mukherjee A, Chandrasekaran N (2011). Cytogenetic and genotoxic effects of zinc oxide nanoparticles on root cells of *Allium cepa*. *J Hazard Mater* 190: 613-621.
- Kumari M, Mukherjee A, Chandrasekaran N (2009). Genotoxicity of silver nanoparticles in *Allium cepa*. *Sci Total Environ* 407: 5243-5246.
- Lee WM, Kwak JI, An YJ (2012). Effect of silver nanoparticles in crop plants *Phaseolus radiatus* and *Sorghum bicolor*: media effect on phytotoxicity. *Chemosphere* 86: 491-499.
- Ma X, Geiser-Lee J, Deng Y, Kolmakov A (2010). Interactions between engineered nanoparticles (ENPs) and plants: phytotoxicity, uptake and accumulation. *Sci Total Environ* 408: 3053-3061.
- McShan D, Ray PC, Yu H (2014). Molecular toxicity mechanism of nanosilver. *J Food Drug Anal* 22: 116-127.
- Mittler R (2002). Oxidative stress, antioxidants and stress tolerance. *Trends Plant Sci* 7: 405-410.
- Nair PMG, Chung IM (2015). Physiological and molecular level studies on the toxicity of silver nanoparticles in germinating seedlings of mung bean (*Vigna radiata* L.). *Acta Physiol Plant* 37: 1719.
- Nair PMG, Chung IM (2014a). Physiological and molecular level effects of silver nanoparticles exposure in rice (*Oryza sativa* L.) seedlings. *Chemosphere* 112: 105-113.
- Nair PMG, Chung IM (2014b). Assessment of silver nanoparticle-induced physiological and molecular changes in *Arabidopsis thaliana*. *Environ Sci Pollut Res* 21: 8858-8869.
- Nakano Y, Asada K (1981). Hydrogen peroxide is scavenged by ascorbate specific peroxidase in spinach chloroplasts. *Plant Cell Physiol* 22: 867-880.
- Oukarroum A, Barhoumi L, Pirastru L, Dewez D (2013). Silver nanoparticle toxicity effect on growth and cellular viability of the aquatic plant *Lemna gibba*. *Environ Toxicol Chem* 32: 902-907.
- Panda KK, Achary VMM, Krishnaveni R, Padhi BK, Sachindra SN, Surendra SN, Brahma PB (2011). In vitro biosynthesis and genotoxicity bioassay of silver nanoparticles using plants. *Toxicol In Vitro* 25: 1097-1105.
- Patlolla AK, Berry A, May L, Tchounwou PB (2012). Genotoxicity of silver nanoparticles in *Vicia faba*: a pilot study on the environmental monitoring of nanoparticles. *Int J Environ Res Public Heal* 9: 1649-1662.
- Pokhrel LR, Dubey B (2013). Evaluation of developmental responses of two crop plants exposed to silver and zinc oxide nanoparticles. *Sci Total Environ* 452-453: 321-332.
- Porra RJ (2002). The chequered history of the development and use of simultaneous equations for the accurate determination of chlorophylls a and b. *Photosynth Res* 73: 149-156.
- Qian H, Peng X, Han X, Ren J, Sun L, Zhengwei F (2013). Comparison of the toxicity of silver nanoparticles and silver ions on the growth of terrestrial plant model *Arabidopsis thaliana*. *J Environ Sci* 25: 1947-1956.
- Ravindran A, Prathna TC, Verma VK (2012). Bovine serum albumin mediated decrease in silver nanoparticle phytotoxicity: root elongation and seed germination assay. *Toxicol Environ Chem* 94: 91-98.
- Saed-Moucheshi A, Shekoofa A, Pessaraki M (2014). Reactive oxygen species (ROS) generation and detoxifying in plants. *J Plant Nutr* 37: 1573-1585.
- Sharma P, Bhatt D, Zaidi MGH, Saradhi PP, Khanna PK, Arora S (2012). Silver nanoparticle-mediated enhancement in growth and antioxidant status of *Brassica juncea*. *Appl Biochem Biotechnol* 167: 2225-2233.
- Song U, Jun H, Waldman B, Roh J, Kim Y, Yi J, Lee EJ (2013). Functional analyses of nanoparticle toxicity: a comparative study of the effects of TiO₂ and Ag on tomatoes (*Lycopersicon esculentum*). *Ecotoxicol Environ Saf* 93: 60-67.
- Sukumaran S, Grant A (2013). Effects of genotoxicity and its consequences at the population level in sexual and asexual *Artemia* assessed by analysis of inter-simple sequence repeats (ISSR). *Mutat Res - Genet Toxicol Environ Mutagen* 757: 8-14.
- Thuesombat P, Hannongbua S, Akasit S, Chadchawan S (2014). Effect of silver nanoparticles on rice (*Oryza sativa* L. cv. KDML 105) seed germination and seedling growth. *Ecotoxicol Environ Saf* 104: 302-309.
- Unal D, Silah H (2013). Genotoxicity effects of Flusilazole on the somatic cells of *Allium cepa*. *Pestic Biochem Physiol* 107: 38-43.
- Vannini C, Domingo G, Onelli E, Mattia FD, Bruni I, Marsoni M, Bracale M (2014). Phytotoxic and genotoxic effects of silver nanoparticles exposure on germinating wheat seedlings. *J Plant Physiol* 171: 1142-1148.
- Yasur J, Rani PU (2013). Environmental effects of nanosilver: impact on castor seed germination, seedling growth, and plant physiology. *Environ Sci Pollut Res Int* 20: 8636-8648.
- Zietkiewicz E, Rafalski A, Labuda D (1994). Genome fingerprinting by simple sequence repeat (SSR)-anchored polymerase chain reaction amplification. *Genomics* 15: 176-83.

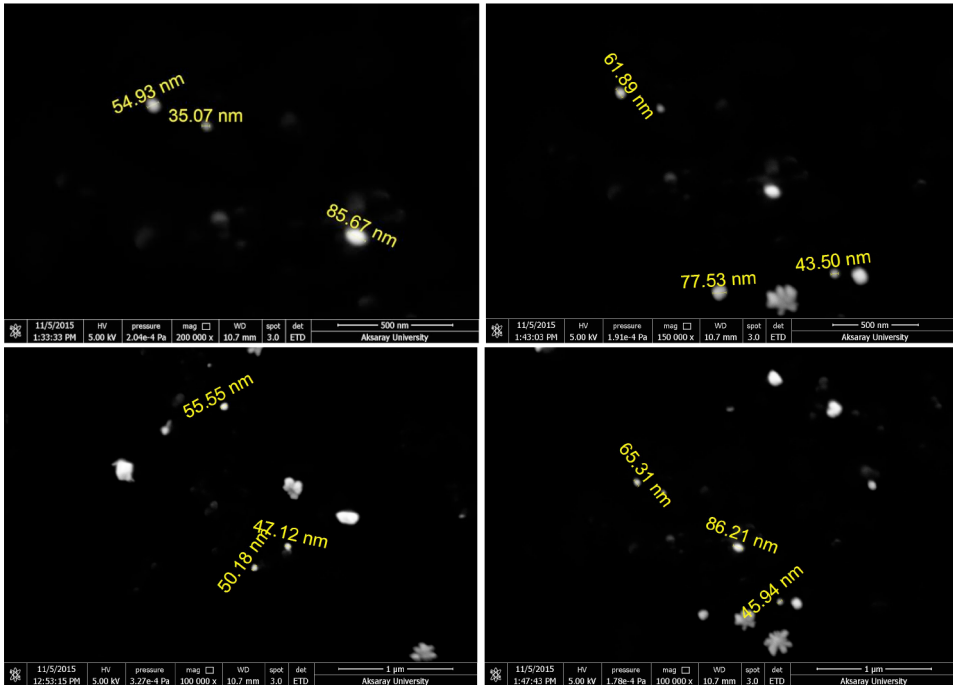


Figure S1. SEM images of silver nanoparticles.

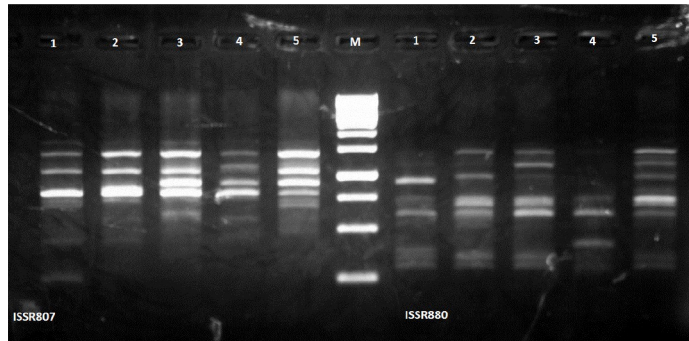


Figure S2. ISSR 807 and ISSR 880 profiles of *S. lycopersicum* L. treated with various concentration of AgNPs. Lane 1: control, Lane 2: 10 mg/L AgNPs, Lane 3: 20 mg/L AgNPs, Lane 4: 40 mg/L AgNPs, Lane 5: 80 mg/L AgNPs, and Lane M: 1kb DNA ladder.